

Abstract

Adaptive GMAW pipeline welding is a specialized application of adaptive GMAW technology for welding pipelines in the oil and gas industry. The technology utilizes real-time monitoring and feedback control systems to adjust welding parameters based on pipeline geometry, material properties, and environmental conditions. The adaptive GMAW pipeline welding process can increase welding efficiency, reduce weld defects, and enhance weld quality. The technology has become increasingly important in the oil and gas industry due to the high demands for pipeline infrastructure, and the need for cost-effective, efficient, and high-quality welding solutions. Nevertheless, challenges still must be overcome such as laser tracking accuracy in orbital welding system due retroactive movements in function of offset between laser TCP and torch TCP, and rail base surface error. This work aimed to develop a calibration methodology for increasing the accuracy over an adaptative orbital welding system. The main results show that previous joint mapping using Laser at TCP can be used to create a correction curve to mitigate the surface error due to the relation among rail, pipe and laser offset.

1. Introduction

Pipeline welding is a specialized form of welding used in the construction, maintenance, and repair of pipelines that transport various substances such as oil, gas, and water over long distances. These pipelines are typically made of high-strength steel and require welding techniques that meet strict safety and quality standards. Nevertheless, pipeline welding involves a variety of welding processes, including Gas Metal Arc Welding (GMAW), Shielded Metal Arc Welding (SMAW), Flux-Cored Arc Welding (FCAW), and Submerged Arc Welding (SAW). The selection of welding process depends on the thickness of the pipe, the type of material being welded, and the environmental conditions in which the welding is being performed.

One of the critical aspects of pipeline welding is the weld quality, which is essential to ensure the structural integrity and safety of the pipeline. Weld defects such as porosity, undercutting, and lack of fusion can lead to pipeline failures, which can result in environmental damage, property damage, and even loss of life. To ensure high-quality welds, pipeline welders must undergo specialized training and certification. Welders must be familiar with welding codes and standards, such as the American Petroleum Institute (API) 1104 Welding Code for Pipelines and ASME Boiler and Pressure Vessel Code (Jeff, 2013).

Pipeline welding requires high skill and expertise, as it often involves working in remote locations and adverse weather conditions. Pipeline welders must also be aware of the potential hazards of working with high-pressure pipelines and take appropriate safety precautions, in addition, due to these complicated environments, even specialized welders under these conditions are susceptible to making mistakes, therefore, to avoid these problems and promote safety both mechanized and automatized welding can be a suitable alternative to perform with robustness and repeatability these operations.

In general, orbital welding automation present a tendency to improve the welding productivity. However, constant monitoring and corrections by the operators are necessary due to the systematic variations of the process, such as the distortions generated in the joint preparation, resulting from the bevel machining or joint assembly. These variations can be translated as variations in the position and joint opening, besides of concentricity and cylindricity, among other dimensional variations. These distortions affect the welding process stability and torch positioning, which cannot be kept

constant throughout the entire process as discussed by Bae, Lee & Ahn (2002). Thus, pipeline automated welding operations that require real-time correction still need direct action by the operator/welder on the parameters (current, voltage, wire speed) and movement (welding speed, weaving, path) during the welding.

For full welder independence, the welding system needs to emulate not only their manual skills and tacit knowledge about the process but also the cognitive functions applied in the operation. These functionalities are the objective of the integrative technology called adaptive welding, which adds the use of sensors and mechatronic equipment with adequate geometric precision, repeatability, and robustness, as well as artificial intelligence (strategies, routines, control, and correction algorithms). Research has been developed for evaluate suitable sensing system for pipeline welding using vision sensor, arc sensor, infrared sensing, touch sensing and Laser vision sensor. According to Rout, Deepak & Biswall (2019) review found that among complex sensors for joint measurement, the sensor most used in industry and in research is the laser triangulation sensor, because it presents greater precision and resolution in relation to the other sensors, allied with multiple geometry parameters measured within each image. Applying that technology, it can be cited Li, Xu, Yan & Tan (2007) which presents a Cartesian system for welding large-diameter tubes, where the arm has two degrees of freedom and carries a torch and the laser vision system in the effector. This work presents methodologies for online joint tracking, i.e., during processing, which are validated using the submerged arc process.

Besides Marmelo (2012) presented a system for the adaptive orbital welding of narrow gap-type joints, using a laser triangulation sensor as a source of information to feed the algorithm developed. The system was composed of the integration of three main modules, a Serimax Saturnax 5 orbital welding manipulator, a Lincoln welding source, using the GMAW-P synergic process, and a Mini-I/60 Robot Servo Laser sensor. The results reported show that the system was able to perform automatic welding and joint inspection. The algorithm uses equations developed from regression analysis of empirical tests. In addition, Kindermann, Silva & Dutra (2015) investigated the use of sensors for real-time correction in orbital welding, where an anthropomorphic robot was used to conduct the torch. The sensors for joint monitoring were an arc sensor and a sensor based on electrical contact. Based on this hardware, algorithms to generate an automatic orbital trajectory and welding parameterization were developed. The proposed strategy and torch control by the arc sensor were validated by means of deposits on pipe specimens. The root pass welding was performed using the short-circuit controlled GMAW process together with the arc sensor. The main problem encountered was the need for constant oscillation of the welding torch as a function of the operational arc sensor characteristics.

Despite the above-mentioned studies, many challenges still must be overcome regarding the implementation of adaptive orbital welding for large tubes. For instance, there is a lack of information over the real sources of uncertainties associated with the system, restraining the improvement of repeatability and accuracy. For this, specific adaptive algorithms for orbital welding, as well as a method for checking and calibrating errors arising from the mobile-based manipulator are proposed.

The present work aimed improve the applicability of an automated orbital welding system for pipeline building by integrating a vision system (laser triangulation sensor), in order to continuously control the process (real time), as a proper adaptive welding system should. For this, it was necessary to develop algorithms capable of performing seam tracking with robots that are assembled over the pipeline, a situation particularly difficult because the robot's rail suffers deformations according to the pipe's geometry, demanding a systematic error calibration of the rail's form.

2. Experimental procedure

Initially, the communication and integration of the system components was carried out. These consist of the SPS Tartilope V3 orbital welding manipulator, IMC A7 welding source and the Metavision SLS50 V1 laser triangulation sensor. In this assembly the laser sensor was placed at 30 mm in front the welding torch, to avoid the arc luminosity, following the manufacturer's recommendations. This distance between the laser line and the torch was called “offset”. The experimental setup used is shown in Figure 1.

Figure 1 – Components of the orbital welding system developed in this study.

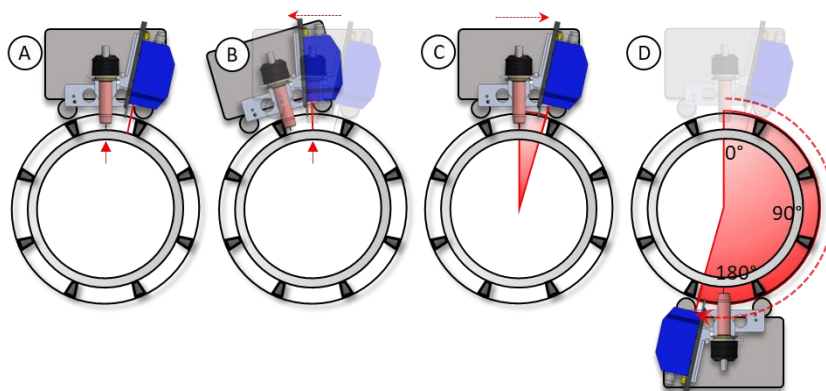


Source: Produced by the author.

The algorithm developed is constantly fed with information from manipulator and laser sensor at a rate of 25 Hz. The manipulator provides data related to the position (X, Y and Z) for every 0.2 mm traveled over a rail (X). The laser sensor provides information on the joint geometry, where the root gap is the main parameter of interest. Based on an ROI, which in this case was defined as the center of the groove, the algorithm calculates the torch position deviations in the movement along the X direction and welding parameters (current, wire feed speed, weaving parameters) based on neural network.

As previously described, given the need for a lag between the laser sensor and the welding torch due to the influence of the electric arc, a 30 mm displacement of the torch in relation to the laser sensor was used. This layout required previous scanning of the region between the laser sensor and the torch, which is referred to as the offset. Initially the manipulator moves 30 mm in the opposite direction to the welding (exactly the offset value), the region is scanned until the offset is zero and the corrected path is executed. The scheme in Figure 2 illustrates the offset reading procedure. This previous scan stores information related to ROI and tool center point (TCP) in a buffer, as well as information on the correction to be applied (point by point).

Figure 2 – Schematic example of offset scanning: A) torch on TCP in P0; B) manipulator recoil; C) offset scanning; and D) process execution.

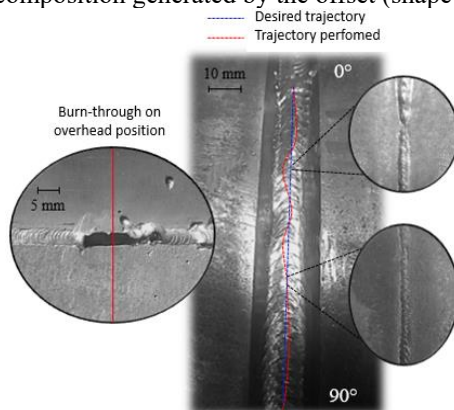


Source: Produced by the author.

The algorithm receives the position (X, Y and Z) from both the TCP and ROI, with TCP position being informed by the manipulator and the ROI by the laser sensor. The sum of these points (TCP and ROI position) results in a point that represents the correct TCP position on the ROI (groove center). These points represent the path that must be executed by the torch to maintain the TCP over the ROI, i.e., the joint trajectory correction map. Due to the difference in sensor acquisition frequency and manipulator weaving frequency, Y Path values/y position values read oscillate around a mean curve. To attenuate this noise, a low-pass filter (exponential smoothing) is used, which softens the reading of the manipulator movement.

By means of this logic it is possible to act on the position of the welding torch to keep it aligned with the center of the joint, adding the relative difference between the sensor reading and the desired axis of movement. However, due to the design of the system, which is similar to that described by Chen, Dharmawan, Foong & Song (2018), in which the manipulator base moves on a rail coupled to a segment of pipe, there is a shape error arising from the pipe and rail composition as a function of the offset (distance between torch and laser sensor). This error makes the welding process more sensitive, generating unpredictable oscillations in the movement of the welding torch relative to the information obtained by the sensor. This, in turn, generates unacceptable welding defects from the perspective of the established minimum quality requirements, as shown by the example of welding without correcting this shape error given in Figure 3.

Figure 3 – Example of failure generated by a deviation in the path as a function of the error associated with the rail and tube composition generated by the offset (shape error).

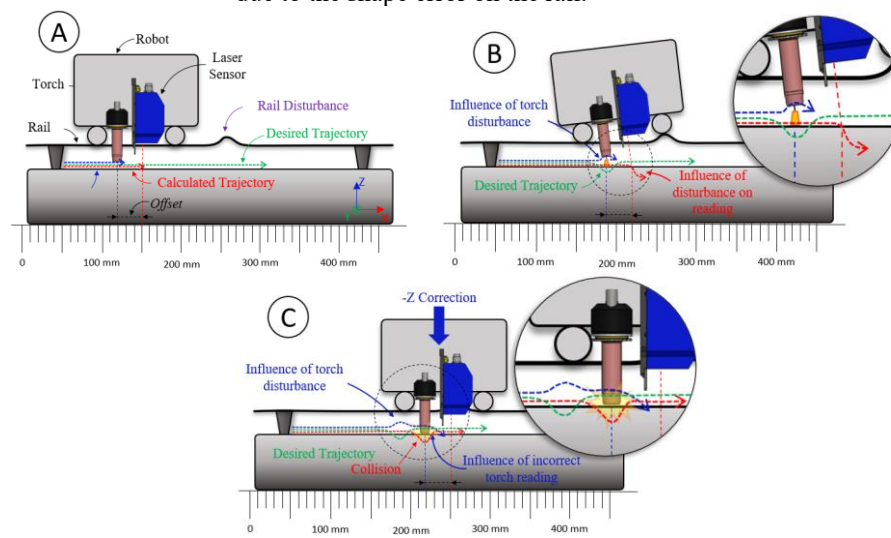


Source: Produced by the author.

Therefore, as described by Chen, Dharmawan, Foong & Song (2018), Yang, Liu, Peng & Liang (2020) and Hou, Xu, Xiao & Chen (2020), it is necessary to initially carry out the calibration of the

system, that is, to map the shape error present in the rail. The error could be visualized, following the procedure: (1) Scan the joint with the torch at the TCP (Laser sensor 30 mm ahead); (2) Scan the joint with the laser sensor in place of the torch, i.e., at the TCP. In this way, it is possible to verify the retroactive influence of the shape error on the path carried out by the welding torch. The idea scenario would be that the two curves show the same trajectory as the path on which the manipulator moves, without shape error. However, there was divergence in the curves obtained in the tests performed due retroactive shape error. These errors are a systematic component of the rail and tube composition (ovalization, ripples and surface defects), generated by the offset. The Figure 4 schematically represents the effect of this error on the path.

Figure 4 – Representation of the shape error as a function of the offset on the path, where: A) system in undisturbed mode; B) disturbance in the path generated by a shape error on the rail; and C) retroactive effect on the path due to the shape error on the rail.

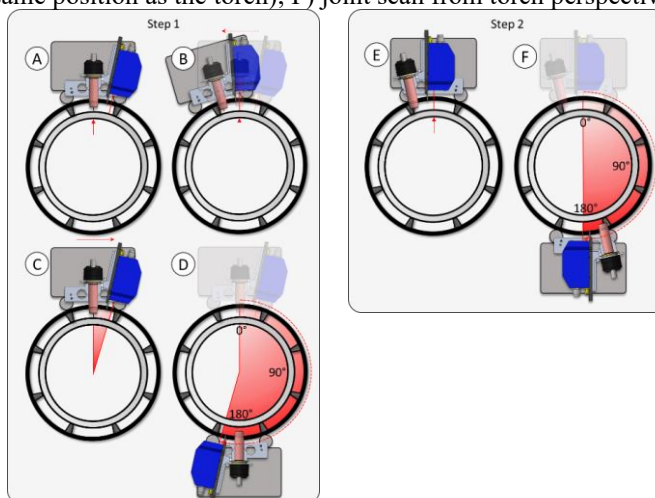


Source: Produced by the author.

The developed calibration method focuses on scanning the joint with the Laser sensor in place of the welding torch and vice-versa. The difference between the scans obtained is the systematic error of the system which can be added to the path created in real time with the sensor in its real position. This method tends to attenuate the deviations generated by the rail and tube composition, which are connected to the offset.

To execute the calibration step, i.e., shape error compensation, the following procedure is proposed. Firstly, scan the joint with the measurement offset (torch at the TCP) and, secondly, scan the joint with the laser at the TCP. Figure 7 shows a flowchart of the calibration and execution steps of the process.

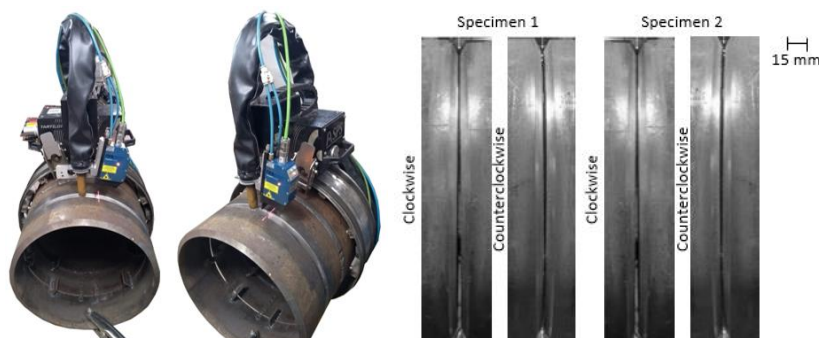
Figure 7 – Flowchart of the adaptive welding process developed, where STEP 1: A) torch positioning at part zero; B) back of the system for offset compensation; C) reading the offset; D) scanning the joint; and STEP 2: E) laser at TCP (same position as the torch); F) joint scan from torch perspective.



Source: Produced by the author.

Validation tests were performed on both the joint tracking and the adaptive parameterization algorithm based on AI. In these tests, pipe specimens were made from API 5L grade B steel pipe segments with 12” diameter and ½” thickness were used, with the aforementioned single V-groove with 30° bevel, in addition, was used variable root opening between 1 mm and 4.5 mm. Figure 8 shows the experimental setup used in the final welding tests, showing that geometric regularity was achieved on the assembly of the specimens.

Figure 8 – The experimental setup used for the welding tests.

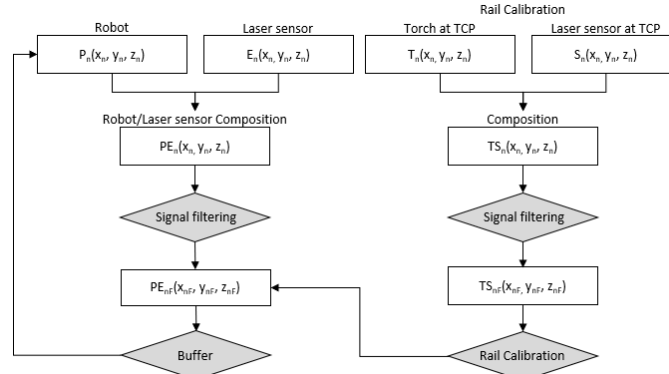


Source: Produced by the author.

3. Final Remarks

The algorithm developed applies a correction that is composed by the laser tracking (real time) added to the difference between the two readings performed, which compensates the error associated with the rail. The rail’s form is a random component of the system because it varies from joint to joint in a random manner. The path control algorithm identifies the point as a function of the X coordinate and applies the corrections on the Y and Z axes. The flowchart in Figure 9 illustrates the algorithm with the compensation of the rail shape error. From this calibration, it is possible to start the welding process with closed-loop control, in order to avoid anomalies arising from the thermal effect of the welding or former unpredictable movement deviations.

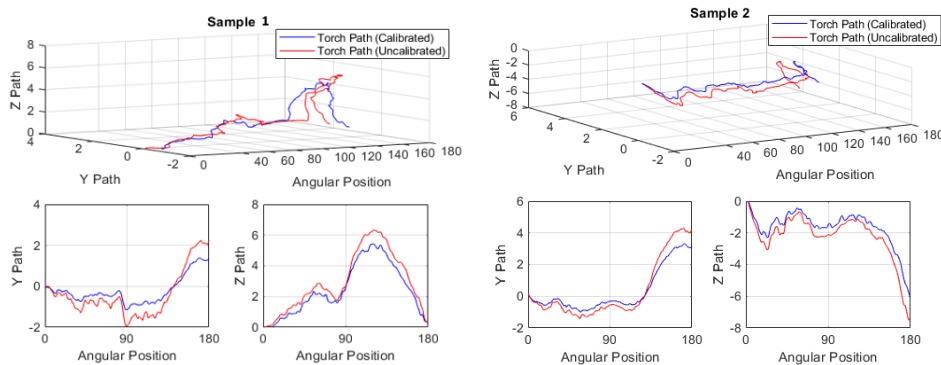
Figure 9 – Flowchart of position correction algorithm with rail compensation.



Source: Produced by the author.

In the validation tests with the application of the rail shape error calibration, a clear improvement in the process was noted, since the influence of this error on the process was considerably reduced, and it became independent of the operator during operation. The operator functions as a supervisor in this type of system. The difference between the methods (with and without calibration) can be seen in the graphs in Figure 10. These show two examples of trajectories carried out with the system, where it is possible to observe the difference, highlighting the importance of knowing the system error sources.

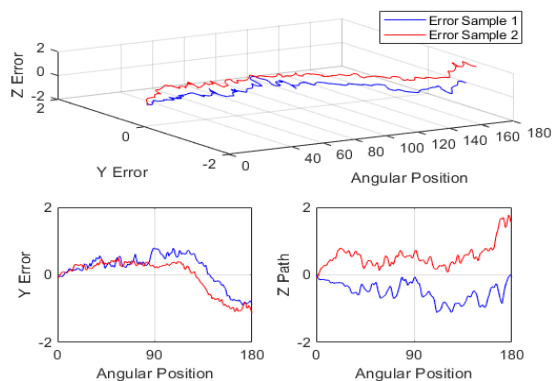
Figure 10 – Graph of torch path calibrated and uncalibrated.



Source: Produced by the author.

The difference between the paths read with the torch at the TCP and with the laser sensor at the TCP represents the error associated with the composition formed by the pipe and rail. This shape error is described in Figure 11 for two different specimens (Samples 1 and 2). In the case of Sample 1 there was a maximum error of 1.8 mm for the Z axis and 1.4 mm for the Y axis while for Sample 2 there was a maximum error of 3.2 mm for the Z axis and 1.5 mm for the Y axis. The nature of this error is random and inherent to the process, however, it can be predicted using this method. From this error curve it is possible to carry out the compensation by associating it with the online correction map generated by the algorithm.

Figure 11 – Graphs showing error in torch paths obtained with calibrated and uncalibrated methods.

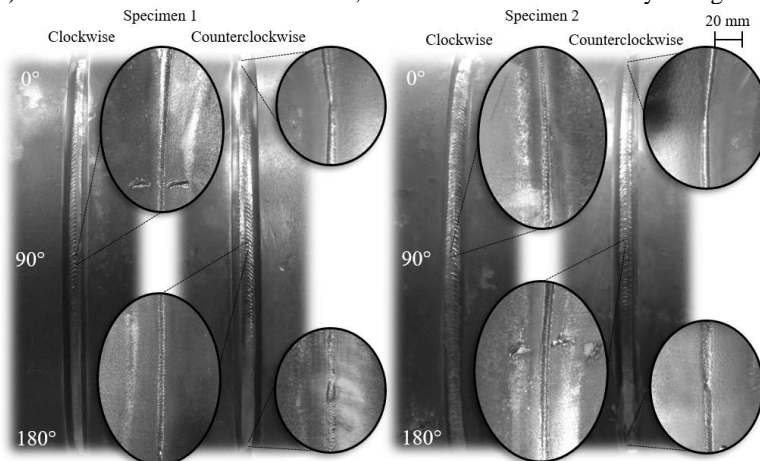


Source: Produced by the author.

The shape error is the difference between the methods (calibrated and uncalibrated paths) and a correction of up to 2 mm was observed, as shown in Figure 11. Although these values may appear to be small, they have a strong influence because the sensitivity of the process is high. Thus, small variations can be highly detrimental to the process, especially in the case of advanced processes, such as welding pipes for the oil and gas industry. These results validate the proposed algorithm for rail shape calibration, as well as its potential for pipe welding operations or any other type of demand where the manipulator is installed over the weld specimen.

The system developed and enhanced in this work, as well as the proposed algorithms (for seam tracking, rail shape calibration and adaptive welding) showed good results, not just in theory but also by the test specimen welded as can be noticed in Figure 12.

Figure 12 - Results obtained for the adaptive orbital welding algorithm (when present, transversal marks aside the root (bottom) view welds are not a weld defect, but marks of the C assembly fixing accessory).



Source: Produced by the author.

The algorithm for rail shape calibration demonstrated its usefulness in situations where the manipulator is installed over the weld specimen. In this case, it's common for its rail to deform, resulting in random torch movement during welding if these distortions are not compensated. The proposed algorithm may also be used for rail calibration of welding cells upon installation, consisting of an algorithm with full capability of delivering a good result for this task also. Welding inspection apparel that uses rails or the base metal as its track can also benefit from the proposed algorithm for the offset/rail/base calibration. As a previous scan was implemented in order to calibrate the rail

deformation, this algorithm allows single laser line projection sensors to be utilized for this functionality.

The adaptive welding algorithm developed with neural network methods also showed promising results, being able to adapt the parameters for the gap variations presented within the range of groove geometry variability and pipe alignment. The methods for obtaining the inputs for this algorithm were also compiled, encouraging other researcher to use this method as a starter point for further own developments. The methods have also potential to be applied in the metal-mechanic industry in general due to its increased robustness if compared to mechanized welding, and so not restricted for large pipe diameter welding applications.

4. Acknowledgments

The research proposed in this paper was supported by Labsolda - Mechatronic and Welding Institute, Federal University of Santa Catarina, SPS, IMC and Petrobras.

5. References

Jeff N (2013) Maximizing pipeline welding efficiency. *Welding Journal*. Miami, Florida. 92(6):74-78. ISSN 0043-2296.

Bae KY, Lee TH, Ahn KC (2002) An optical sensing system for seam tracking and weld pool control in gas metal arc welding of steel pipe. *Journal of Materials Processing Technology* 120(1-3):458 – 465. [https://doi.org/10.1016/S0924-0136\(01\)01216-X](https://doi.org/10.1016/S0924-0136(01)01216-X)

Rout A, Deepak BBVL, Biswal BB (2019) Advances in weld seam tracking techniques for robotic welding: A review. *Robotics and Computer Integrated Manufacturing*, 56:12-37.

<https://doi.org/10.1016/j.rcim.2018.08.003>

Li Y, Xu D, Yan Z, Tan M (2007) Girth Seam Tracking System Based on Vision for Pipe Welding Robot. In: Tarn TJ., Chen SB., Zhou C. (eds) *Robotic Welding, Intelligence and Automation*. Lecture Notes in Control and Information Sciences. 362:391-399. https://doi.org/10.1007/978-3-540-73374-4_47

Marmelo PC (2012) Real Time Evaluation of Weld Quality in Narrow Groove Pipe Welding. Phd Thesis. Cranfield University.

Kindermann RM, Silva RHG, Dutra JC (2015) Development and Validation of Algorithms Employed for Sensor Systems in Robotic Orbital Root Pass Welding of Pipelines. *International Welding*. 20(4):391-402. <https://doi.org/10.1590/0104-9224/SI2003.08>

Chen X, Dharmawan AG, Foong S, Song Soh GS (2018) Seam tracking of large pipe structures for an agile robotic welding system mounted on scaffold structures. *Robotics and Computer-Integrated Manufacturing*. 50:242-255. <https://doi.org/10.1016/j.rcim.2017.09.018>

Yang L, Liu Y, Peng J, Liang Z (2020) A novel system for off-line 3D seam extraction and path planning based on point cloud segmentation for arc welding robot. *Robotics and Computer Integrated Manufacturing*. 64:1-14. <https://doi.org/10.1016/j.rcim.2019.101929>

Hou Z, Xu Y, Xiao R, Chen S (2020) A teaching-free welding method based on laser visual sensing system in robotic GMAW. *Int J Adv Manuf Technol* 109:1755–1774. <https://doi.org/10.1007/s00170-020-05774-0>